Analysis of the radial and tangential stress distribution between two neighbouring circular holes under internal pressure by numerical modelling

by Sh. Arshadnejad* and K. Goshtasbi†

Synopsis

Stress analysis in a rock medium is essential to determine the stress concentration between two consecutive circular holes and prediction of fracture behaviour. When two consecutive circular holes in a hard rock medium such as granite are loaded internally by the pressure of non-explosive expansion material (NEEM), stress concentration occurs between the holes which then causes the rock to fracture. In this work, finite element (FE) analysis using Phase2 code was employed to study the stress concentration between two consecutive circular holes under internal pressure induced by NEEM. Effects of different hole diameters and spacings, rock properties and NEEM pressures have been analysed. The data gained from the numerical analysis and analytical solutions were then used to develop two models. These models were then modified by using the FE data and polynomial regression analysis. The developed analytical models showed to be in a very good agreement with the FE analysis. Hence, the developed models can be used with confidence to determine stress distribution and concentration factors around two consecutive circular holes in a hard and brittle rock which are loaded internally by the pressure induced from the NEEM.

Keywords
Finite element method, non-explosive, quarry mining, stress concentration..

Introduction

One of the main methods in quarry mining, especially in hard rocks, is the controlled fracture method that is carried out by the introduction of a slowly advancing crack by non-explosive expansion material (NEEM). The application of NEEM in hard rock quarry mining has recently been increased[1]. This method of rock breakage is without noise and vibrations and its operation, compared to the blasting method, is more controllable, very safe and easy and without extra undesirable cracks in the rock block.

In this method, some circular holes are drilled consecutively with equal length, diameter and spacing (centre to centre distance) in a rock block. Subsequently, the holes are filled with NEEM, which by its expansion will generate an incremental static load into the holes after about two to four hours[1–5]. If the spacing of the holes is suitable, it will create a crack between two consecutive holes, and the rock will fracture along the high-stress concentration path between the holes. If the material of the medium is brittle, such as hard rocks (e. g. granite and quartzite), it will not yield and no plastic behaviour in the material before failure will be observed[6–13]. Thus, the material is considered to behave in a linear elastic mode.

When there are two consecutive holes in a plate loaded internally, stress concentration will occur. The maximum elastic stresses (stress concentration) were examined by several methods, such as photoelastic analysis[14,15], direct strain measurement[16,17] and numerical modelling[18,19]. There are many empirical models for estimating stress concentration in different geometry, such as a circular hole. The scope of this work is to develop a model to analyse stress concentration between two consecutive circular holes in a hard rock medium which is loaded internally by NEEM. The model, based on analytical method and verification by the finite element method, has been upgraded.

Stress distribution around a circular hole due to internal and external loads

Stress distribution around a circular hole depends on the stress field condition. Kirsch[20] initially studied this problem for a single circular hole under two-direction stress field.

* *Department of Mining Engineering, Mahallat Branch, Islamic Azad University, Mahallat, Iran.*

† *Department of Mining Engineering, Tarbiat Modares University, Tehran, Iran.*

 SA ISSN 0038–223X/3.00 + 0.00. Paper received Feb. 2009; revised paper received Feb. 2011.

Analysis of the radial and tangential stress distribution

The stress distribution of a thick wall cylinder under uniform external and internal loading is as follows[21]:

$$\sigma_r = \frac{\left(a^2P_i - b^2P_o\right)}{b^2 - a^2} + \frac{a^2b^2\left(P_i - P_o\right)}{r^2\left(b^2 - a^2\right)} \quad [1]$$

$$\sigma_\theta = \frac{\left(a^2P_i - b^2P_o\right)}{b^2 - a^2} - \frac{a^2b^2\left(P_i - P_o\right)}{r^2\left(b^2 - a^2\right)} \quad [2]$$

where σ_r and σ_θ are the radial and tangential stresses respectively and r is the radial distance of the consider point from hole centre. P_i and P_o are internal and external pressures respectively and a and b are the internal and external radius of the thick wall cylinder respectively. Because of axial symmetry in the loadings and body geometry, there is no shear stress in the medium. As a principle in rock mechanics, the tension stress is considered negative and the compressive stress is considered positive[22,23]. The constraint for using thick wall cylinder equations is as follow[24,25]:

$$\frac{b-a}{a} > \frac{1}{20} \quad [3]$$

If there is no external pressure ($P_o = 0$) the equations become:

$$\sigma_r = \frac{a^2P_i}{b^2 - a^2}\left(1 + \frac{b^2}{r^2}\right) \quad [4]$$

$$\sigma_\theta = \frac{a^2P_i}{b^2 - a^2}\left(1 - \frac{b^2}{r^2}\right) \quad [5]$$

If the thickness of the cylinder wall increases to infinity ($b \to \infty$), the cylinder will transform into a circular hole in an infinite plate, such as a hole in a rock medium. Then, Equations [4] and [5] convert to:

$$\lim_{b\to\infty}\sigma_r = \frac{a^2P_i}{r^2} = P_i\left(\frac{a}{r}\right)^2 \quad [6]$$

$$\lim_{b\to\infty}\sigma_\theta = -\frac{a^2P_i}{r^2} = -P_i\left(\frac{a}{r}\right)^2 \quad [7]$$

Stress concentration factors around a circular single hole due to uniform and axial symmetrical external pressure were analysed by Howland[26], Frocht[27], Lipson and Juvinall[28]. Obert and Duvall[29] have studied the stress distribution around pillars (rock columns) between two parallel circular excavations subjected to uniaxial compressive external loading by photoelasticity method. If the type of external loading is tension in two directions, two empirical models were developed by Schulz[30] and Peterson[31].

Stress concentration between consecutive holes under internal pressure

When two or more circular holes in a plate are loaded by internal pressure, stress concentration will occur among them. When the stress intensity is equal to the rock fracture toughness, cracks may be initiated. Subsequently, the crack will grow; however, as the length of the crack increases, the stress on the crack tip decreases, due to distancing from the hole, thus decreasing the stress concentration. Nevertheless, by increasing the stress induced from the hole due to application of NEEM, in due time, the stress intensity on the crack tip will again increase up to the level of rock fracture toughness. Thus, again the crack will grow further, and this circle of events will repeat; hence, a controllable mechanism for crack growth may be achieved. Figure 1 shows a rock fracture between two neighboring holes due to the application of the NEEM in a granite quarry mine in Taleghan, Iran.

As stated before, Equations [6] and [7] may be used to determine the stress distribution around a circular hole. However, when there are two consecutive circular holes in a rock medium, these equations have to be modified. The modified equations may be assumed to be as follows:

$$\sigma_r = C_r.P_i\left(\frac{a}{r}\right)^2 \quad [8]$$

$$a = \frac{d}{2} \Rightarrow \sigma_r = C_r.P_i\left(\frac{d}{2r}\right)^2 \quad [9]$$

Figure 1—Rock fracture between two neighboring holes by the NEEM in a granite mine (Arshadnejad, 2010)

Analysis of the radial and tangential stress distribution

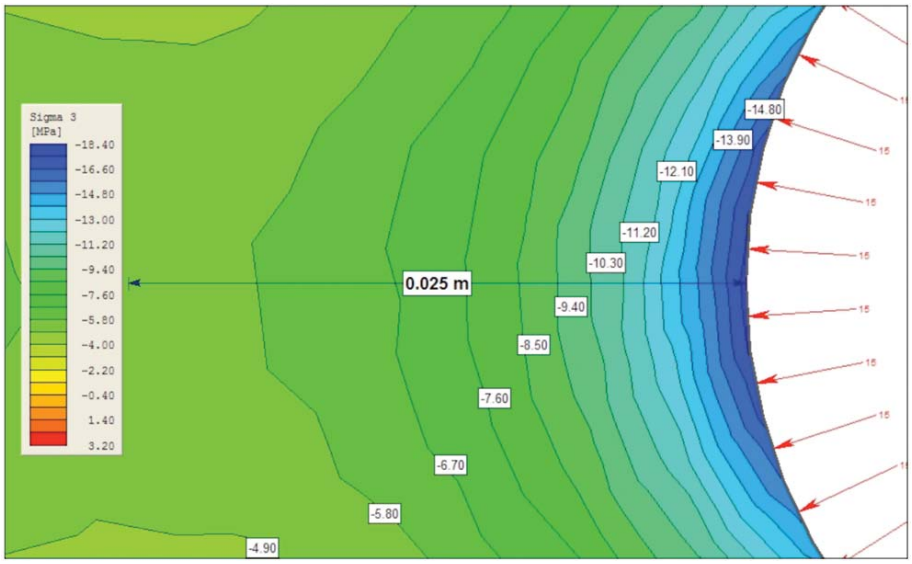

Figure 2—Trajectories stress on nodal points in the numerical modelling

Table I

Applied parameters in the numerical modelling

Hole diameter (mm)	Hole spacing (mm)	Poisson's ratio	Internal pressure by NEEM (MPa)
28, 32, 38, 44	50, 80, 110, 140, 170, 200, 230, 260, 290	0.1, 0.15, 0.2, 0.25, 0.3	10, 20, 30, 40, 60, 80, 100

$$\sigma_\theta = -C_\theta . P_i \left(\frac{d}{2r}\right)^2 \quad [10]$$

where C_r and C_θ are the stress concentration factors for the radial and tangential elastic stress respectively and d is the diameter of holes. Other parameters are those explained earlier in Equations [1] and [2].

In this work, the Phase2 code[32,33] based on the finite element method (FEM) was used to determined the radial and tangential stresses around the hole (σ_r and s_θ) by numerical analysis. In this respect, six nodal triangular elements with nodal averages were utilized. Figure 2 shows the iso-stress contours around of a hole.

The model geometry and the parameters were selected based on real conditions of quarry mining operations. There is a new experimental model which it can be used for determining of the NEEM's pressure (Arshadnejad, 2010).

$$P_i = 0.566 t^{0.933} d^{0.407} E^{0.493} \quad [11]$$

Where P_i is the NEEM's Pressure in MPa, t is the time of loading in hours, d is the hole diameter in m and E is the Young's modulus of the rock or material in GPA.

Table I shows the parameters that were applied in the numerical models. The internal pressures in the holes were due to non-explosive expansion material (NEEM).

While running the program, it was noticed that Young's modulus and internal pressure have no effect on the stress concentration factors. Since the stress concentration factor is essentially of geometrical characteristics, this finding seems to be justified. However, Poisson's ratio tends to have some effect, as it has been confirmed by previous work[34]. Therefore, just around 180 numerical models had to be analysed. Figure 3 shows the stress concentration zones between two consecutive circular holes with a typical hole diameter of 44 mm and hole spacing of 50 mm under internal pressure of 15 MPa due to NEEM.

The results from numerical analysis show that Poisson's ratio, hole diameters and hole spacings are the main parameters that affect the stress concentration between two consecutive circular holes. The data from numerical analysis, along with multiple regression and logarithmical data[35,36], were used to determine C_r and C_θ. Equations [12] and [13] show these predicted models.

$$C_r = 1.0352 \left(\frac{d}{S}\right)^{0.001} \upsilon^{0.015} \quad [12]$$

$$C_\theta = 1.1715 \left(\frac{d}{S}\right)^{0.124} \upsilon^{-0.025} \quad [13]$$

where υ is the Poisson ratio of rock, d is the diameter of holes and S is the edge-to-edge distance between two consecutive holes (hole spacing). Figures 4 and 5 show a comparison between finite element (FE) data and predicted models from Equations [9] and [10] for the radial and tangential stresses versus distance from hole centre.

Modification of the predicted models

With reference to Figures 4 and 5, it can be observed that stresses determined from FE data and predicted models are

Analysis of the radial and tangential stress distribution

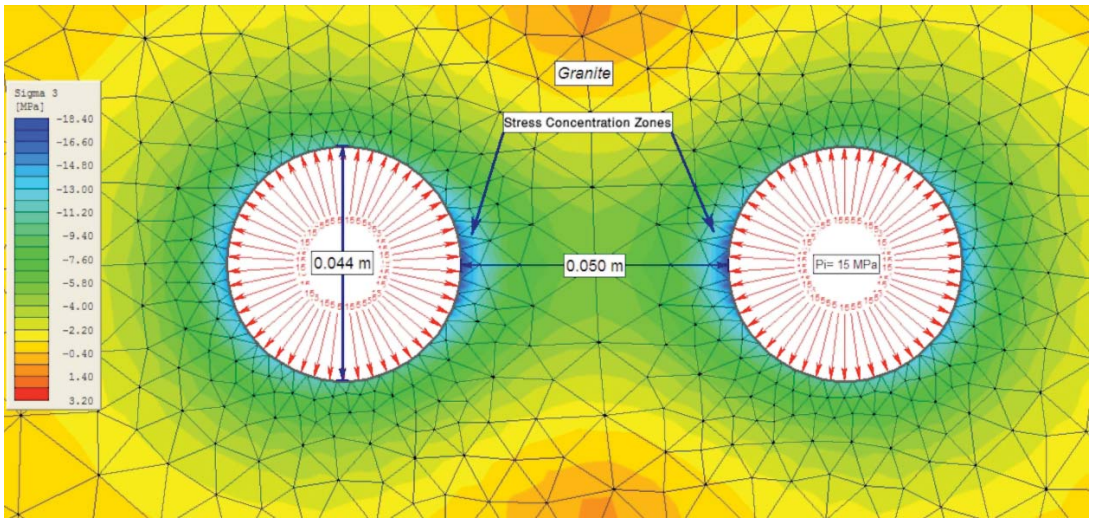

Figure 3—Stress concentration zones between two consecutive holes

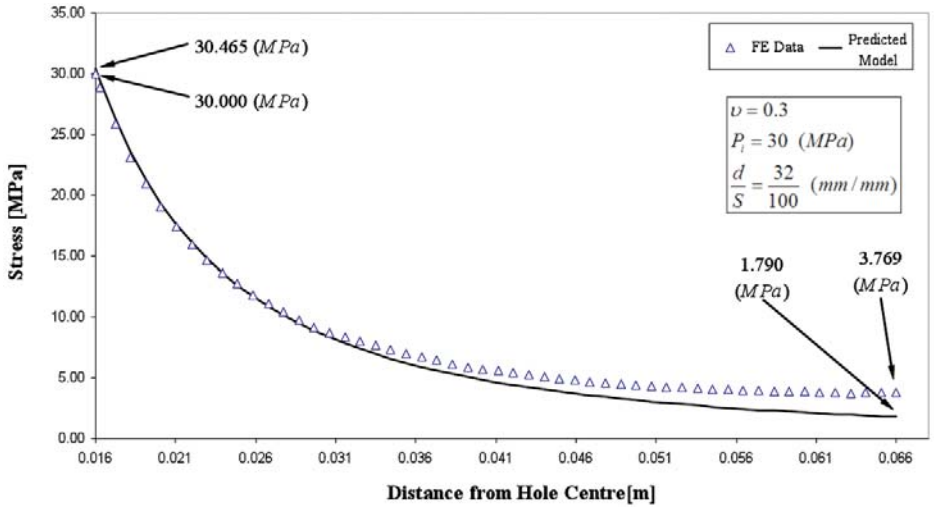

Figure 4—Radial stress distribution at vicinity of a circular hole from FE data and predicted model

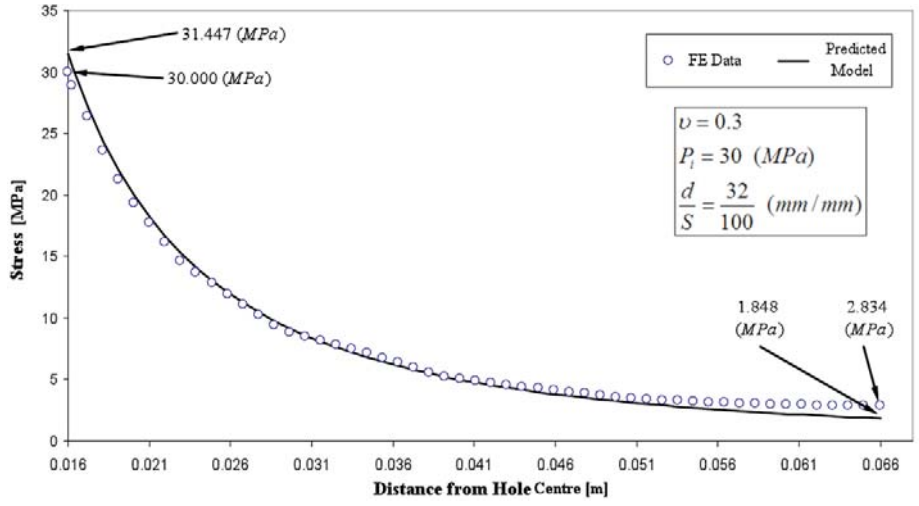

Figure 5—Tangential stress distribution at vicinity of a circular hole from FE data and predicted model

not quite similar and there are some differences between those. Hence, modifications have to be applied to the predicted models so that a closer agreement can be achieved. The values of differential stresses (the difference in FE data and predicted models) were plotted against the distance from hole centre for both of the radial and tangential stresses. The polynomial regression analysis was then utilized as a modification function and applied to the results given in Figures 6 and 7. The modified models achieved from this analysis are shown in Equations [14] and [16]. The corresponding modified functions are also demonstrated by Equations [15] and [17].

$$\sigma_r = C_r.P_i\left(\frac{d}{2r}\right)^2 + f(r) \quad [14]$$

$$f(r) = 17390r^3 - 2569.5r^2 + 163.62r - 2.6522 \quad r^2 = 0.9942 \quad [15]$$

$$\sigma_\theta = -[C_\theta.P_i\left(\frac{d}{2r}\right)^r + f'(r)] \quad [16]$$

$$f'(r) = 60397r^3 - 7878.2r^2 + 351.67r - 5.1152 \quad r^2 = 0.9421 \quad [17]$$

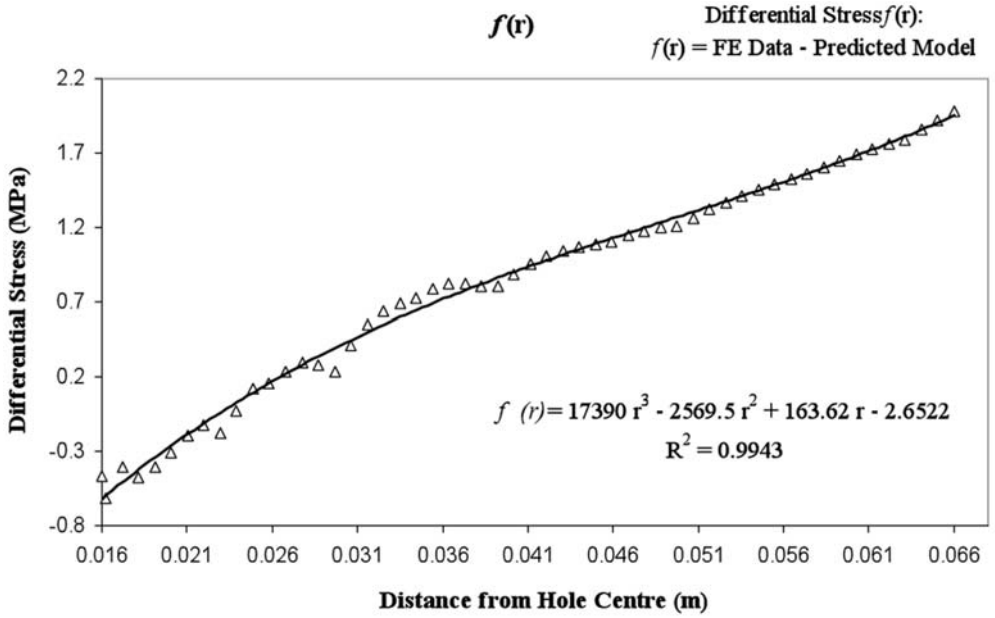

Figure 6—Differential radial stress against the distance from hole centre

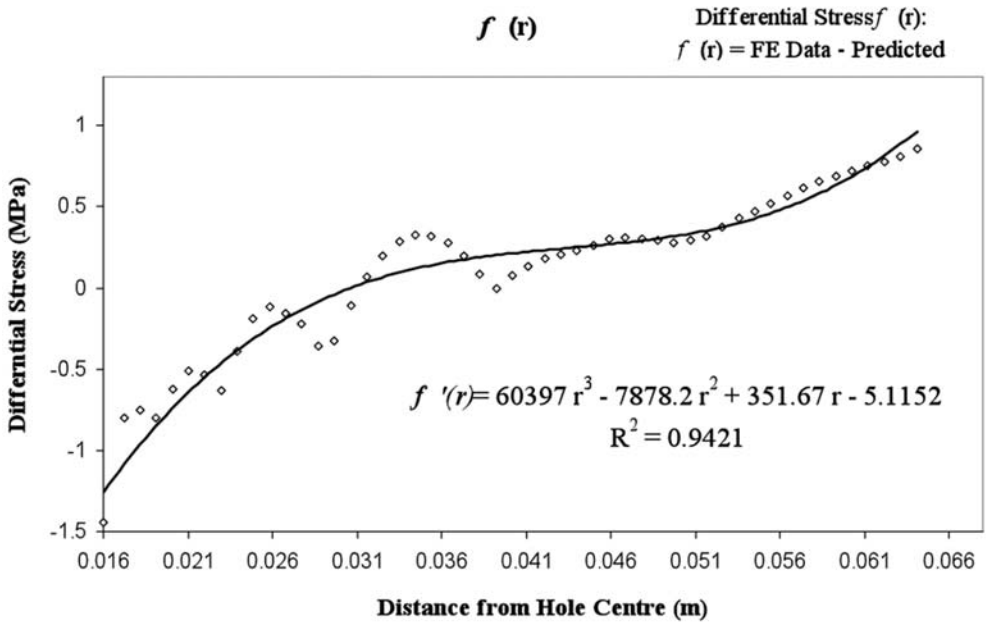

Figure 7—Differential tangential stress against the distance from hole centre

Analysis of the radial and tangential stress distribution

A comparison was then made between the FE data, predicted models (Equations [9] and [10]) and modified models (Equations [14] and [16]) in Figures 8 and 9 by plotting the corresponding radial and tangential stresses versus the distance from hole centre. As it is anticipated, the values obtained from FE data and modified models are almost identical; apparently the values of the predicted models show some deviation.

Therefore, the final equations for determining stress distribution including stress concentration factor between consecutive circular holes due to internal pressure of NEEM are as follow:

$$\sigma_r = 1.0352\left(\frac{d}{S}\right)^{0.001} \upsilon^{0.015}.P_i\left(\frac{d}{2r}\right) + \left[17390r^3 - 2569.5r^2 + 163.62r - 2.6522\right] \quad [18]$$

$$\sigma_\theta = -[1.1715\left(\frac{d}{S}\right)^{0.124} \upsilon^{-0.025}.P_i\left(\frac{d}{2r}\right)^2 + (60397r^3 - 7878.2r^2 + 351.67r - 5.1152)] \quad [19]$$

where d, r and S are in meters and P_i, σ_r and σ_θ are in *MPa*. Finally, verification was done by plotting stresses from modified models versus FE data. Figures 10 and 11 show these validation graphs. It is observed that there is a remarkable agreement between the results.

Conclusions

Based on the solution for a thick wall cylinder and assuming that the wall thickness increases to infinity, an equation for determining stress around a single circular hole in a rock plate maybe achieved. In this work, this equation has been

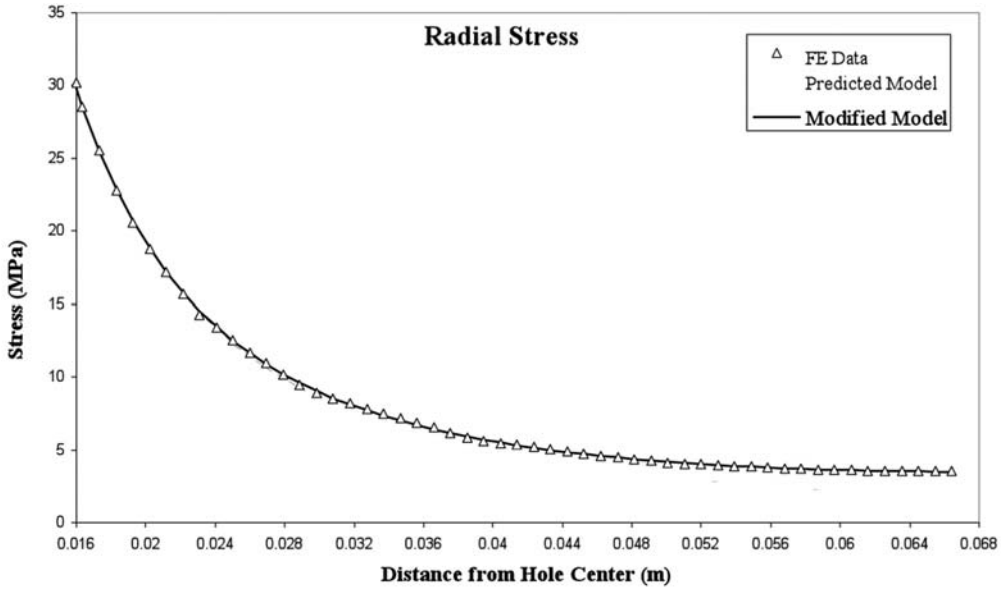

Figure 8—Modified model and FE data for radial stress distribution

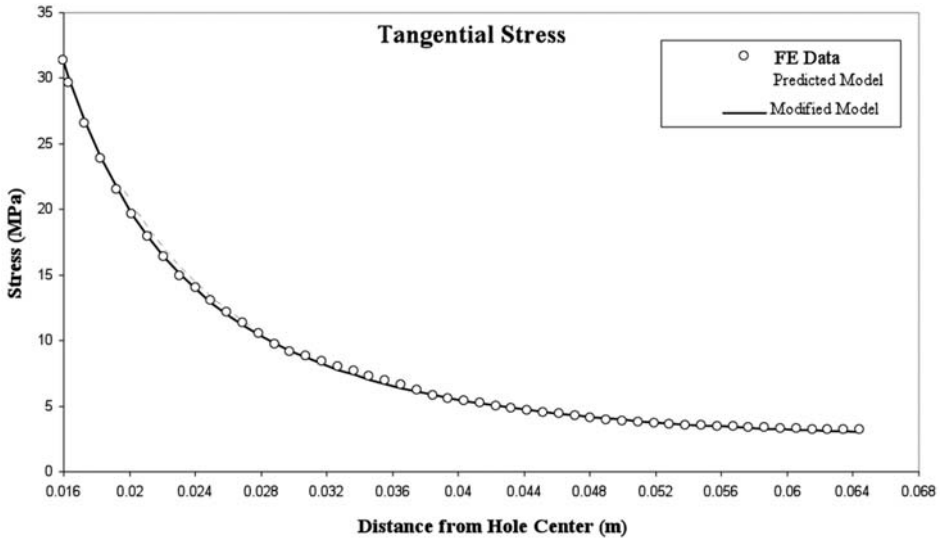

Figure 9—Modified model and FE data for tangential stress distribution

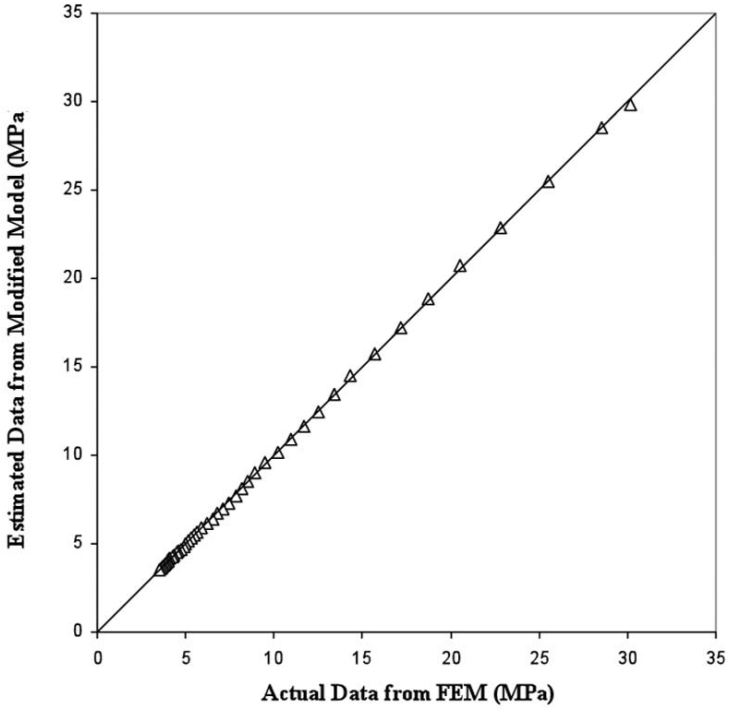

Figure 10—Actual data and estimated data for the radial stress distribution

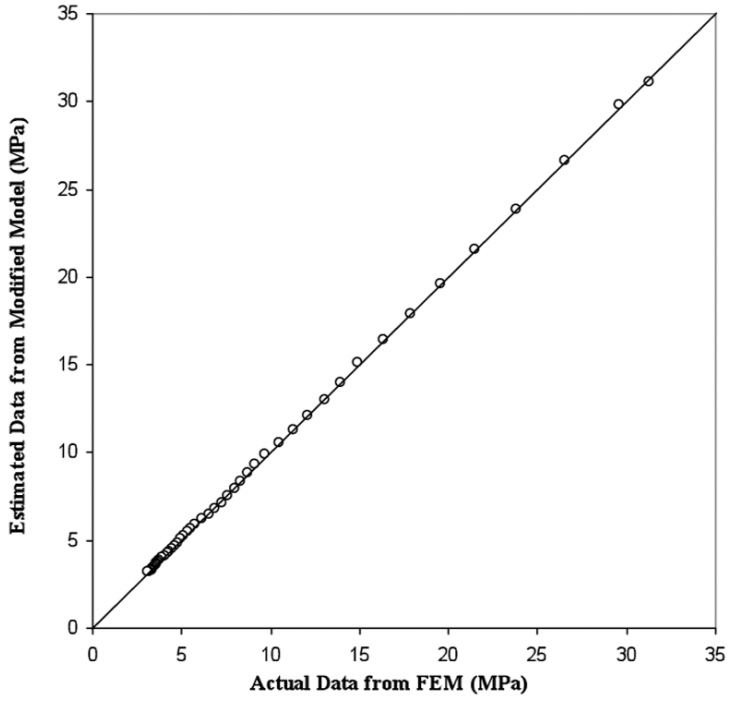

Figure 11—Actual data and estimated data for the tangential stress distribution

modified for determining the stress concentration between two consecutive circular holes by introducing a coefficient in the equation. This stress concentration coefficient was estimated by numerical modelling based on the model geometry and Poissons ratio, resulting in two equations that are obtained by multiple regression analysis. Due to differences in the stresses determined from FE data and the models, appropriate modifications using polynomial regression analysis were applied in order to achieve a closer agreement between the results. Therefore, the obtained relations can be used confidently to determine stress distribution between two consecutive circular holes internally pressurized by NEEM in a hard and brittle rock medium such as granite.

References

1. Arshadnejad, Sh., A model for analysis of rock fracture in granite due to non-explosive expansion material. PhD Thesis, Azad University, Tehran, Iran, 2010, 173 p.

2. Zhangzhe, J., Hong, L., and Wen, Zh. Splitting mechanism of rock and concrete under expansive pressure, *Conference of Demolition and Reuse of Concrete and Masonry*, vol. 1, Demolition method and practice (RILEM), Y. Kasai, (ed.) Nihon University, Japan, 1988, pp. 141–148.

3. Goto, K., Kojima, K., and Watabe, K. The mechanism of expansive pressure and blow-out of static demolition agent, *Conference of Demolition and Reuse of Concrete and Masonry*, vol. 1, Demolition method and practice (RILEM), Y. Kasai, (ed.) Nihon University, Japan, 1988, pp. 116–125.

4. Jana, S. Non-explosive expanding agent—an aid for reducing environmental pollution in mines, *Indian Mining and Engineering Journal*, 1991, pp. 31–35.

5. Hayashi, H., Soeda, K., Hida, T., and Kanbayashi, M. Non-explosive demolition agent in Japan, *Conference of Demolition and Reuse of Concrete* (RILEM), Erik K. (ed.) Lauritzen, London,1994, pp. 231–241.

6. Hoek, E. and Bieniawski, Z.T. Brittle rock fracture propagation in rock under compression, *Int. J. Fracture Mechanics*, vol. 1, no. 3, 1965, pp. 137–155.

7. Lajtai, E.Z. Effect of tensile stress gradient on brittle fracture initiation, *Int. J. Rock Mech. & Min. Sci.*, vol. 9, 1972, pp. 569–578.

8. Lawn, B.R. and Wilshaw, T.R. *Fracture of brittle solids*, Cambridge University Press, Cambridge, UK, 1975.

9. Ingraffea, A.R. and Schmidt, R.A. Experimental verification of a fracture mechanics model for tensile strength prediction of Indiana limestone, *Proceeding of 19th US Symp. on rock Mechanics*, 1978, pp. 247–253.

10. Fowell, R.J. Suggested method for determining mode I fracture toughness using cracked chevron notched Brazilian disc (CCNBD) specimens, ISRM Commission on Testing Methods, *Int. J. Rock Mech. Min. Sci.*, vol. 32, no. 1, 1995, pp. 57–64.

11. Eberhardt, E., Stimpson, B., and Stead, D. The influence of mineralogy on the initiation of microfractures in granite, *Proceeding of 9th International Congress on Rock Mechanics*, Paris. G. Vouille and P. Berest, (eds.) A.A. Balkema, Rotterdam, 1999, pp. 1007–1010.

12. Orekhov, B.G. and Zertsalov, M.G. *Fracture Mechanics of Engineering Structures and Rocks*, A. A. Balkema, 2001.

13. Yagiz, S. Assessment of brittleness using rock strength and density with punch penetration test, *Journal of Tunnelling and Underground Space Technology*, vol. 24, 2009, pp. 66–74.

14. Hoek, E. and Bieniawski, Z.T. Application of the photoelastic coating technique to the study of the stress redistribution associated with plastic flow around notches, *S. Afr. Mech. Eng.* vol. 12, no. 8, 1963, pp. 22–226.

15. Joussineau, Gh. D., Petit, J. P., and Gauthier, B. D. M. Photoelastic and numerical investigation of stress distributions around fault models under biaxial compressive loading conditions, *Journal of Tectonophysics*, vol. 363, 2003, pp. 19–43.

16. Nesetova, V. and Lajtai, E. Z. Fracture from compressive stress concentrations around elastic flaws, *Int. J. Rock Mech. & Min. Sci.*, vol. 10, 1973, pp. 265–284.

17. Chong, K.P., Harkins, J.S., Kuruppu, D.M., and Leskinen, A.I.L. Strain rate dependent mechanical properties of western oil shale, *Proceeding of 28th US Symp. on Rock Mechanics,* 1987, pp. 157–164.

18. Bazant, Z.P. Crack band model for fracture and geomaterials, *Numerical methods in geomechanics proc.*, Edmonton, 1982, pp. 1137–1152.

19. Yan, X. Rectangular tensile sheet with single edge crack or edge half-circular-hole crack, *Journal of Engineering Failure Analysis*, vol. 14, 2007, pp. 1406–1410.

20. Kirsch, G. Die theorie der elastizitat und die bedurfnisse der festigkeitslehre, *Veit. Ver. Deut. Ing.*, vol. 42, 1898, pp. 797–807.

21. Timoshenko, S.P. and Goodier, J.N. *Theory of Elasticity*, McGraw-Hill, New York, 1951.

22. Hoek, E. and Brown, E.T. *Underground excavations in rock*, The institution of mining and metallurgy, London, 1980.

23. Goodman, R.E. *Introduction to rock mechanics*, 2nd edition, John Wiley and Sons, New York, 1989.

24. Shigley, J.E. *Machine Design*, McGraw-Hill, 1956.

25. Hertzberg, R.W. *Deformation and fracture mechanics of Engineering materials*, John Wiley & Jons, Inc., 1996.

26. Howland, R.C.J. On the stress in the neighborhood of a circular hole in a strip under tension, *Trans. Roy. Soc.*, London, A., vol. 229, 1929.

27. Forcht, M.M. Factors of stress concentration photoelastically determined, *Trans. ASME, Ap. M.*, vol. 57, 1935, pp. A–67.

28. Lipson, Ch. and Juvinall, R. *Handbook of stress and strength design and material applications*, The Macmillan Company, New York, 1963.

29. Obert, L. and Duvall, W.I. *Rock mechanics and the design of structures in rock*, John Wiley & Sons, New York, 1967.

30. Schulz, K.J. On the state of stress in perforated strips and plates, *Proceeding of Neth. Roy. Acad. Sci.*, vols. 45 to 48, 1942.

31. Peterson, R.E. *Stress concentration design factors*, John Wiley & Sons, Inc., New York, 1974.

32. Rocscience, Inc., Phase2 Verification manual, Version 2.1, 1999.

33. Rocscience, Inc., Phase2 model program reference manual, 2001.

34. Zienkiewicz, O.C. *The finite element method in engineering science*, Second edition, McGraw-Hill, London, 1971.

35. Chatfield, Ch. *Statistics for technology*, 3th edition, Chapman & Hall, 1983.

36. Montgomery, D.C., Runger, G.C., and Hubele, N.F. *Engineering statistics*, Second edition, John Wiley & Sons, Inc., 2001. ◆